Analysis of Compliance Characteristic for Effective Multi-fingered Robotic Peg-In-Hole Task

Byoung-Ho Kim°,†, Sang-Rok Oh†, Byung-Ju Yi°, Il Hong Suh°, and Wan Kyun Chung‡

° : School of Electrical Eng. and Computer Science, Hanyang Univ., Seoul, Korea
† : Intelligent System Control Research Center, KIST, Seoul, Korea
‡ : School of Mechanical Eng., POSTECH, Pohang, Korea
(E-mail: bj@email.hanyang.ac.kr)

Abstract

This paper deals with analysis of the compliance characteristic for effective peg-in-hole task using robot hand without inter-finger coupling. We first classify the task of inserting a peg-in-a-hole into three contact styles between the peg and the hole. Next, we analyze the conditions of the specified stiffness matrix in the operational space to successfully and more effectively achieve the given peg-in-hole task for each case. It is concluded that the location of compliance center on the peg and the coupling stiffness element between the translational and the rotational direction play important roles for successful peg-in-hole task. Simulation results are included to verify the feasibility of the analytic results.

Keywords : *Peg-in-hole, Analysis of compliance characteristic, Robot hand.*

1 Introduction

When an object grasped by a robot hand is being manipulated, explicit force-based fine motion control [1]-[3] may not be practically easy because it is not only hard to implement the force sensor, but also the signal processing of the force signal is not easy. It therefore has been pointed out that instead of explicit force signal the stiffness or compliance is an important quantity for characterizing the grasping and manipulation of robot hands in the case that it is specially dominated by approximated linear analysis where low velocities and small relative motions lead to small inertial forces.

Many approaches have been reported in the field of grasp stiffness or compliance [4]-[8]. The stiffness of objects grasped by virtual springs was analyzed in cases of planar and three-dimensional space in [4]. Yoshikawa, et al. [5] proposed a direct compliance control method and applied the method to a parallel arm. In [6], the effective grasp stiffness was analyzed by considering the structural compliances of fingers, fingertips, servo gains at the joints of finger, and small changes in the grasp geometry. And an object-based stiffness control approach have been proposed in [7]. Recently, Kim, et al. [8] proposed an independent finger/joint-based compliance control method for robot hands manipulating an object, and also the geometric condition for successful implementation of compliance control scheme have been addressed. They showed that an independent finger/joint-based compliance control via redundant actuation was more adequate to modulate the operational stiffness comparing with the case of the kinematically redundant structured fingers or manipulators.

In this paper, the independent finger/joint-based compliance control method is applied to a peg-in-hole task using robot hands. Related to the peg-in-hole task using robot hands, Whitney [9] classified the geometry of the inserted peg and analyzed the force relations in the peg-in-hole task by using a remote center compliance mechanism. Asada, et al. [10] analyzed the dynamic process of a peg insertion. Matsuoka, et al. [11] used a multi-sensors-based control system to perform a given peg-in-hole task and also proposed a method of executing tasks based on motion primitives for fine manipulation. Shimoga, et al. [12] presented that the desirable location of compliance center should be that point on the grasped object which first touches or which already is in contact with the inserting work piece. However, the proper location of compliance center and the determination of stiffness characteristics to effectively achieve the given peg-in-hole task have not been considered yet.

In this paper, we first classify the task of inserting a peg-in-a-hole into three contact stylesbetween the peg and the hole. Next, we analyze the conditions of the specified stiffness matrix in the operational space to successfully and more effectively achieve the given peg-in-hole task for each case. By simulations, it is confirmed that the location of compliance center on the peg and the role of a coupling stiffness element existing between the translational andthe rotational direction are important for effective peg-in-hole task.

2 Independent Finger/Joint Based Compliance Control

Consider a rigid peg being inserted in a hole by a three-fingered robot hand in two-dimensional space as shown in Figure 1. The relationship between the

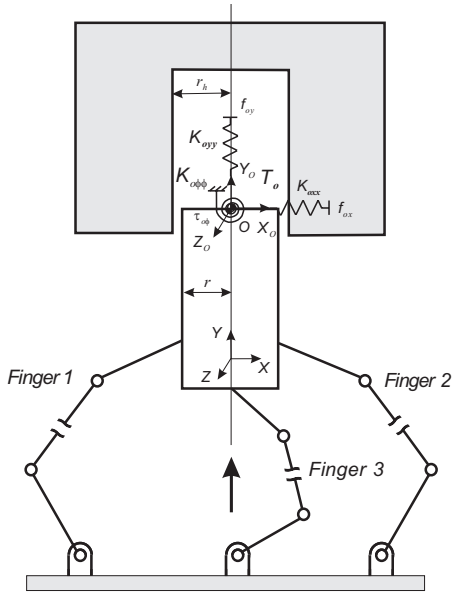

Figure 1: Peg-in-hole task using a three-fingered robot hand.

desired object stiffness matrix $[\boldsymbol{K}_o]$ in the operational space and the stiffness matrix $[\boldsymbol{K}_f]$ in the fingertip space [8] is given as

$$[\boldsymbol{K}_o] = [\boldsymbol{G}_o^f]^T [\boldsymbol{K}_f][\boldsymbol{G}_o^f], \tag{1}$$

where

$$[\boldsymbol{K}_o] = \begin{bmatrix} \boldsymbol{K}_{oxx} & \boldsymbol{K}_{oxy} & \boldsymbol{K}_{ox\phi} \\ \boldsymbol{K}_{oyx} & \boldsymbol{K}_{oyy} & \boldsymbol{K}_{oy\phi} \\ \boldsymbol{K}_{o\phi x} & \boldsymbol{K}_{o\phi y} & \boldsymbol{K}_{o\phi\phi} \end{bmatrix},$$

and $[\boldsymbol{G}_o^f]$ denotes the Jacobian relating the fingertip space to the task space.

In [8], it is analyzed that a robot hand should have at least three fingers to modulate 3×3 object stiffness characteristic in two-dimensionalspace. An alternative form of (1) can be expressed by

$$K_{oo} = [\boldsymbol{B}_f^o]\, K_{ff}, \tag{2}$$

where

$$K_{oo} = [\boldsymbol{K}_{oxx}\ \boldsymbol{K}_{oxy}\ \boldsymbol{K}_{ox\phi}\ \boldsymbol{K}_{oyy}\ \boldsymbol{K}_{oy\phi}\ \boldsymbol{K}_{o\phi\phi}]^T,$$

$$[\boldsymbol{B}_f^o] = \begin{bmatrix} 1.0 & 0.0 & 1.0 & 0.0 & 1.0 & 0.0 \\ 0.0 & 0.0 & 0.0 & 0.0 & 0.0 & 0.0 \\ y_1 & 0.0 & y_2 & 0.0 & y_3 & 0.0 \\ 0.0 & 1.0 & 0.0 & 1.0 & 0.0 & 1.0 \\ 0.0 & -x_1 & 0.0 & x_2 & 0.0 & x_3 \\ y_1^2 & x_1^2 & y_2^2 & x_2^2 & y_3^2 & x_3^2 \end{bmatrix},$$

$$K_{ff} = [{}^1\boldsymbol{K}_{fxx}\ {}^1\boldsymbol{K}_{fyy}\ {}^2\boldsymbol{K}_{fxx}\ {}^2\boldsymbol{K}_{fyy}\ {}^3\boldsymbol{K}_{fxx}\ {}^3\boldsymbol{K}_{fyy}]^T,$$

and y_i, x_i denote the elements of position vectors directing from the ith finger contact position to the task position, and they are given all positive. $[{}^i\boldsymbol{K}_{fxx}]$ and $[{}^i\boldsymbol{K}_{fyy}]$ represent the x- and y-directional stiffness elements in the fingertip space of the ith finger, respectively.

Note that the elements of the second row of the mapping matrix $[\boldsymbol{B}_f^o]$ in (2) are calculated as zero. This is because we excluded the coupling terms ${}^i\boldsymbol{K}_{fxy}(i=1,\ 2,\ 3)$ in the fingertip space for independent compliance control. Thus, we have zero $\boldsymbol{K}_{oxy}$, which, in fact, is a linear combination of ${}^i\boldsymbol{K}_{fxy}(i=1, 2, 3)$. Also, note that the third row of $[\boldsymbol{B}_f^o]$ corresponds to modulation of $\boldsymbol{K}_{ox\phi}$. However, we can easily notice that zero $\boldsymbol{K}_{ox\phi}$ cannot be achieved by all positive stiffness components K_{ff} defined in the fingertip space since the three influence coefficients (i.e., y_1, y_2, and y_3) are always positive in this grasped configuration.

Consider a modified posture of grasp in Figure 2, in which the contact position of the third finger lies above the task position $\boldsymbol{O}$. In this case, the (3, 5) element of $[\boldsymbol{B}_f^o]$ is converted to $-y_3$ and thus, zero $\boldsymbol{K}_{ox\phi}$ can be achieved. However, since the posture of grasp as shown in Figure 2 is not allowed in a peg-in-hole task, zero $\boldsymbol{K}_{ox\phi}$ cannot be obtained. Therefore, $\boldsymbol{K}_{ox\phi}$ always exists.

Let $[\boldsymbol{D}_f^o]$ be the matrix excluding the second and third rows of $[\boldsymbol{B}_f^o]$ and K_{oo}^* be the vector excluding $\boldsymbol{K}_{oxy}$ and $\boldsymbol{K}_{ox\phi}$ of K_{oo}. Then, K_{ff}^* can be obtained as follows:

$$K_{ff}^* = [\boldsymbol{D}_f^o]^+ K_{oo}^*. \tag{3}$$

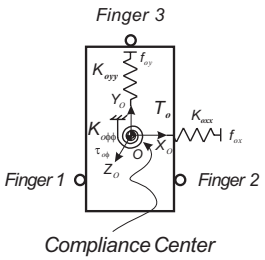

Figure 2: A three-fingered grasp.

Next, the coupling stiffness element $\boldsymbol{K}_{ox\phi}$ can be determined by

$$\boldsymbol{K}_{ox\phi} = [\boldsymbol{B}_f^o]_3 \; K_{ff}^*, \tag{4}$$

where $[\boldsymbol{B}_f^o]_3$ denotes the third row of $[\boldsymbol{B}_f^o]$.

3 Analysis of Compliance Characteristic for Peg-In-Hole Task

The task of inserting a peg-in-a-hole can be classified into three contact styles between the peg and the hole as follows [9]:

1) the case that a left-side of peg is being contacted on the hole,

2) the case that a right-side of peg is being contacted on the hole,

3) the case that the left- and right-sides of peg are simultaneously being contacted on the hole.

In the paper, we consider the peg-in-hole problem in a quasi-static state.

3.1 Left-Side Contact

When a rigid peg being inserted in a hole by three-fingered robot hand in two-dimensional space, let us consider that a left-side of the peg is being contacted on the hole as shown in Figure 3 by x-directional position error and hence the peg is taken some x-directional reaction force.

The forces exerted on the virtual springs attached to the peg tip can be expressed as

$$\begin{bmatrix} f_{ox} \\ f_{oy} \\ \tau_{o\phi} \end{bmatrix} = \begin{bmatrix} \boldsymbol{K}_{oxx} & 0 & \boldsymbol{K}_{ox\phi} \\ 0 & \boldsymbol{K}_{oyy} & 0 \\ \boldsymbol{K}_{o\phi x} & 0 & \boldsymbol{K}_{o\phi\phi} \end{bmatrix} \begin{bmatrix} \delta u_{ox} \\ \delta u_{oy} \\ \delta u_{o\phi} \end{bmatrix}, \tag{5}$$

where the small deflections of the virtual springs in the x-, y-, and rotational directions, respectively, are

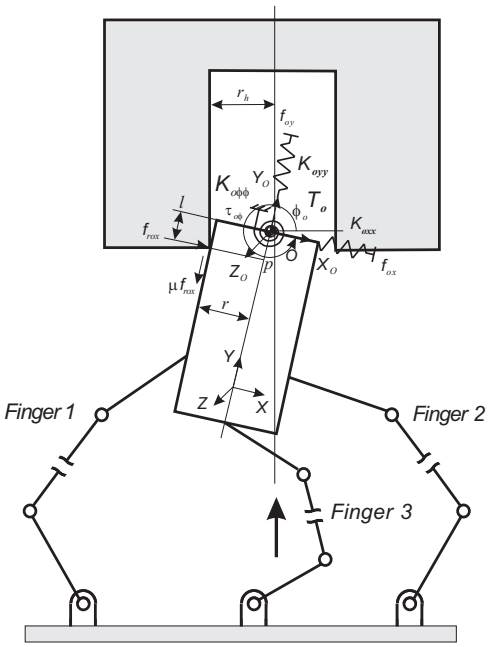

Figure 3: Left-side contact

given by

$$\begin{aligned} \delta u_{ox} &= u_{ox}^d - u_{ox}^a, \\ \delta u_{oy} &= u_{oy}^d - u_{oy}^a, \\ \delta u_{o\phi} &= u_{o\phi}^d - u_{o\phi}^a. \end{aligned}$$

and here u_{oj}^d and u_{oj}^a denote the j-directional desired and actual position, respectively.

The x-directional force f_{ox}, y-directional force f_{oy}, and torque $\tau_{o\phi}$, which are induced by the x-directional reaction force($f_{rox} > 0$), are given by

$$f_{ox} = -f_{rox}, \tag{6}$$
$$f_{oy} = -\mu f_{rox}, \tag{7}$$
$$\tau_{o\phi} = f_{rox}(l + \mu r), \tag{8}$$

where μ, l, and r denote the friction coefficient at the contacting surface, the length between the compliance center and the point p, and the radius of peg, respectively.

If a virtual desired path to be followed is intentionally given to be inside the surface of the hole, the small deflection δu_{ox} of the virtual spring in the x-direction becomes negative. Thus, a positive directional reaction force and its associated friction force are generated, and simultaneously, the orientation change of the peg is occurred by the torque caused by the reaction forces. From equations (5), (6), and (8), the torque

relation at the compliance center can be given by

$$\boldsymbol{K}_{ox\phi}\delta u_{ox} + \boldsymbol{K}_{o\phi\phi}\delta u_{o\phi} = -\boldsymbol{K}_{oxx}(l+\mu r)\delta u_{ox} - \boldsymbol{K}_{ox\phi}(l+\mu r)\delta u_{o\phi}. \quad (9)$$

By rearranging (9), we have

$$\delta u_{o\phi} = -\left\{\frac{\boldsymbol{K}_{ox\phi} + \boldsymbol{K}_{oxx}(l+\mu r)}{\boldsymbol{K}_{o\phi\phi} + \boldsymbol{K}_{ox\phi}(l+\mu r)}\right\}\delta u_{ox}. \quad (10)$$

Note that since the sign of the value inside parenthesis is always given positive and δu_{ox} is negative in this case, the orientation change by touching the left-side of the peg on the hole is at least greater than zero from (10) and hence the inserted peg rotate to the counterclockwise direction about the compliance center. Therefore, this phenomena facilitates the insertion task. Even though l=0 and μ=0, existence of $\boldsymbol{K}_{ox\phi}$ makes the insertion job successful.

3.2 Right-Side Contact

In this section, consider the case that a right-side of the peg is being contacted on the hole as shown in Figure 4.

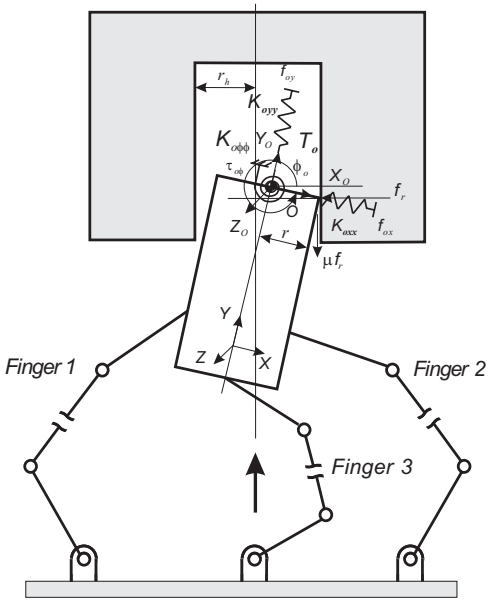

Figure 4: Right-side contact

The forces exerted on the virtual springs of attached to the peg are derived as

$$f_{ox} = f_r\{cos(\phi_o) + \mu sin(\phi_o)\}, \quad (11)$$
$$f_{oy} = -f_r\{sin(\phi_o) + \mu cos(\phi_o)\}, \quad (12)$$
$$\tau_{o\phi} = -r f_{ox}\sigma, \quad (13)$$

where

$$\sigma = -\left\{\frac{tan(\phi_o) - \mu}{1 + \mu tan(\phi_o)}\right\} \geq 0, \quad \phi_{o,min} \leq \phi_o \leq 2\pi,$$
$$\phi_{o,min} = \frac{3\pi}{2} + cos^{-1}\left(\frac{r}{r_h}\right),$$

$\phi_{o,min}$ and r_h denote the minimum orientation angle of the peg and the radius of the hole, respectively.

When a right-side of the peg is being contacted on the hole, some negative directional reaction forces and its associated friction force are generated, and simultaneously, the orientation change of the peg is occurred by the torque caused by the reaction forces. From equations (5), (11), and (13), the torque relation at the compliance center can be given by

$$\boldsymbol{K}_{ox\phi}\delta u_{ox} + \boldsymbol{K}_{o\phi\phi}\delta u_{o\phi} = -r\boldsymbol{K}_{oxx}\sigma\delta u_{ox} - r\boldsymbol{K}_{ox\phi}\sigma\delta u_{o\phi}. \quad (14)$$

By rearranging (14), we have

$$\delta u_{o\phi} = -\left\{\frac{\boldsymbol{K}_{ox\phi} + r\boldsymbol{K}_{oxx}\sigma}{\boldsymbol{K}_{o\phi\phi} + r\boldsymbol{K}_{ox\phi}\sigma}\right\}\delta u_{ox}. \quad (15)$$

From (15), note that the sign of the value inside parentheses is always positive. Since δu_{ox} is always taken positive in this contact type, $\delta u_{o\phi}$ becomes negative. This results clockwise rotation of the peg, which is undesirable for peg insertion.

Now, consider the peg-in-hole task shown in Figure 5, where the location of compliance center is modified. In Figure 5, the length parameters, c and a, and α angle are computed as

$$c = r|tan(\phi_o)|, \quad (16)$$
$$a = \sqrt{r^2 + b^2}, \quad (17)$$
$$\alpha = cos^{-1}\left(\frac{r}{a}\right), \quad (18)$$

where b is the distance from the peg tip to the compliance center and it is a design parameter to be determined.

When we set b larger than c, the x- and y-directional forces, and torque induced by the x-directional reaction force($f_r > 0$) are given by

$$f_{ox} = f_r\{cos(\phi_o) + \mu sin(\phi_o)\}, \quad (19)$$
$$f_{oy} = -f_r\{sin(\phi_o) + \mu cos(\phi_o)\}, \quad (20)$$
$$\tau_{o\phi} = a f_{ox}\lambda, \quad (21)$$

where λ is defined as

$$\lambda = \frac{sin(\alpha) + cos(\alpha)tan(\phi_o) - \mu\{cos(\alpha) - sin(\alpha)tan(\phi_o)\}}{1 + \mu tan(\phi_o)}$$

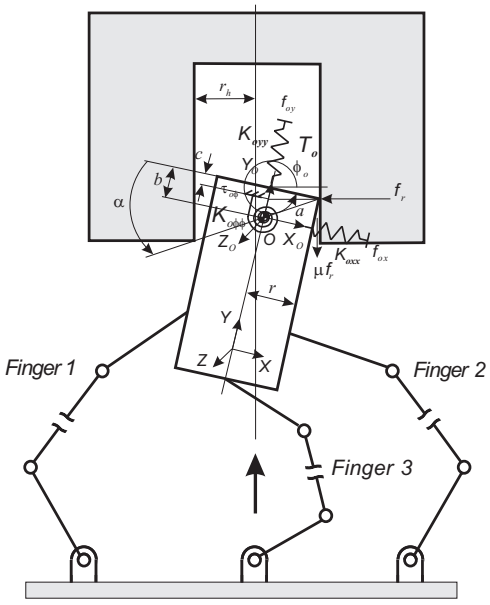

Figure 5: Right-side contact(modified case).

and here, if the α angle is properly determined by setting the distance b, the sign of λ can be set up to be positive in most case.

From equations (5), (19), and (21), the torque relation at the compliance center can be given by

$$\begin{aligned} &\boldsymbol{K}_{ox\phi}\delta u_{ox} + \boldsymbol{K}_{o\phi\phi}\delta u_{o\phi} = \\ &\quad a\boldsymbol{K}_{oxx}\lambda\delta u_{ox} + a\boldsymbol{K}_{ox\phi}\lambda\delta u_{o\phi}. \end{aligned} \tag{22}$$

By rearranging (22), the orientation change of the peg can be expressed as

$$\delta u_{o\phi} = -\left\{\frac{\boldsymbol{K}_{ox\phi} - a\boldsymbol{K}_{oxx}\lambda}{\boldsymbol{K}_{o\phi\phi} - a\boldsymbol{K}_{ox\phi}\lambda}\right\}\delta u_{ox}. \tag{23}$$

In this case, the orientation change of the peg is at least greater than zero if either of the following conditions are satisfied.

$$\begin{aligned} \delta u_{o\phi} &= -\left\{\frac{\boldsymbol{K}_{ox\phi} - a\boldsymbol{K}_{oxx}\lambda}{\boldsymbol{K}_{o\phi\phi} - a\boldsymbol{K}_{ox\phi}\lambda}\right\}\delta u_{ox}, \\ &\boldsymbol{K}_{ox\phi} > a\boldsymbol{K}_{oxx}\lambda \text{ and } \boldsymbol{K}_{o\phi\phi} < a\boldsymbol{K}_{ox\phi}\lambda, \end{aligned} \tag{24}$$

$$\begin{aligned} \delta u_{o\phi} &= -\left\{\frac{\boldsymbol{K}_{ox\phi} - a\boldsymbol{K}_{oxx}\lambda}{\boldsymbol{K}_{o\phi\phi} - a\boldsymbol{K}_{ox\phi}\lambda}\right\}\delta u_{ox}, \\ &\boldsymbol{K}_{ox\phi} < a\boldsymbol{K}_{oxx}\lambda \text{ and } \boldsymbol{K}_{o\phi\phi} > a\boldsymbol{K}_{ox\phi}\lambda. \end{aligned} \tag{25}$$

From equations (24) and (25), we can notice that the stiffness elements in the operational space should be carefully selected for effective handling of the given peg-in-hole task.

Through the above analysis, a similar analysis can be performed for the case that two left- and right-sides of peg are being contacted on the hole.

4 Simulation Results

This section provides simulation results to confirm the orientation change of the peg when the peg contacts the hole. In simulations, we use a three-fingered robot hand equipped with five bar mechanism [8, 13]. The desired stiffness matrix in the operational space is specified as

$$\begin{aligned} \boldsymbol{K}_o &= \begin{bmatrix} \boldsymbol{K}_{oxx} & \boldsymbol{K}_{oxy} & \boldsymbol{K}_{ox\phi} \\ \boldsymbol{K}_{oyx} & \boldsymbol{K}_{oyy} & \boldsymbol{K}_{oy\phi} \\ \boldsymbol{K}_{o\phi x} & \boldsymbol{K}_{o\phi y} & \boldsymbol{K}_{o\phi\phi} \end{bmatrix} \\ &= \begin{bmatrix} 100 & 0 & 1.37 \\ 0 & 1500 & 0 \\ 1.37 & 0 & 0.5 \end{bmatrix}, \end{aligned} \tag{26}$$

where $\boldsymbol{K}_{ox\phi}$ is determined by (4).

The grasp points of the three-fingered robot hand are given $(-x_1, -y_1) = (-0.03, -0.06)$, $(x_2, -y_2) = (0.03, -0.06)$, and $(x_3, -y_3) = (0.0, -0.1)$, where sign of all parameters are set positive and those unit is meter. The material of the peg and the hole is assumed wood. The friction coefficient μ and the initial orientation of the peg are set as 0.3 and 350^o, respectively.

The first simulation corresponds to Figure 3, where the parameter l is fixed as $0.03m$. The second simulation considers the case of Figure 4. the third simulation treats the same task with modified compliance center as shown in Figure 5, where the distance parameter b is set as $0.05m$.

Simulation results are shown in Figures 6, 7, and 8, respectively. Figures 6 shows that the orientation of the inserted peg changes properly upon contacting the left-side of the peg on the hole. Note that the orientation of the peg in the case (a) of Figure 7 decrease for the x-directional deflection, while that of the peg in the case (b) of Figure 7 increase. Consequently, it can be said that the given peg-in-hole task is more easily achieved in the case (b) comparing to the case (a). From Figure 8, it is confirmed that the necessary conditions described in the equation (25) are satisfied during the contact.

From the above analysis, it is concluded that the location of compliance center on the peg should be properly chosen for effective peg-in-hole task and also the coupling stiffness element existing between the x-direction and the rotational direction plays an important role in a peg-in-hole task.

5 Concluding Remarks

In this paper, we analyzed the conditions of the specified stiffness matrix in the operational space to

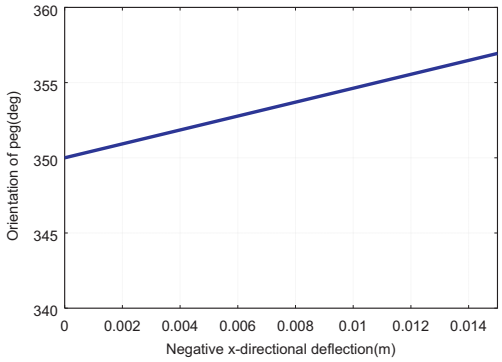

Figure 6: Orientation of the peg for left-side contact.

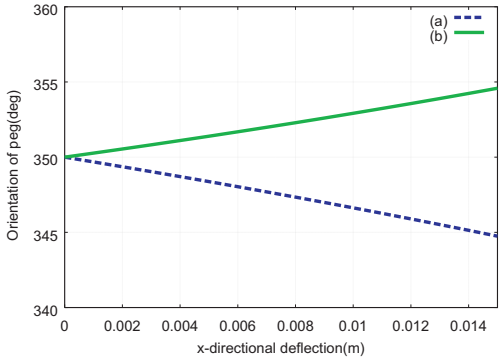

Figure 7: Orientation of the peg for right-side contact: (a) is the case that the compliance center lies in the peg tip and (b) is the case that the location of compliance center is modified.

successfully and more effectively achieve the defined peg-in-hole tasks. Through the analysis, it is concluded that the location of compliance center on the peg and the coupling stiffness element existing between the translational and the rotational direction play important roles for successful insertion task. Further study includes analysis for peg-out-hole problem and 3 dimensional examples.

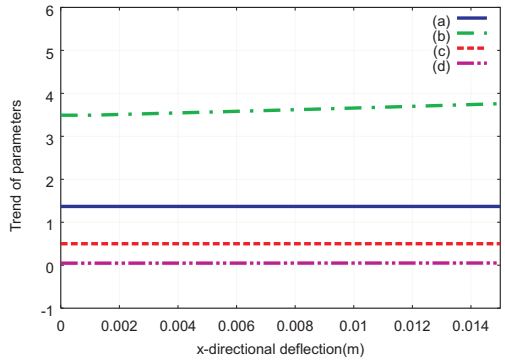

Figure 8: Trend of parameters: (a) $\boldsymbol{K}_{ox\phi}$ (b) $a\boldsymbol{K}_{oxx}\lambda$ (c) $\boldsymbol{K}_{o\phi\phi}$ (d) $a\boldsymbol{K}_{ox\phi}\lambda$.

References

[1] T. Yoshikawa and X. -Z. Zheng, "Coordinated dynamic hybrid position/force control for multiple robot manipulators handling one constrained object," *Int. Jour. of Robotics Research* Vol. 12, No. 3, pp. 219-230, 1993.

[2] T. Hasegawa, T. Matsuoka, T. Kiriki, and K, Honda, "Manipulation of an object by a multi-fingered hand with multi-sensors," *Proc. of Int. Conf. on Industrial Electronics, Control, and Instrumentation*, pp. 174-179, 1996.

[3] H. Maekawa, K. Tanie, and K. Komoria, "Dynamic Grasping Force Control Using Tactile Feedback for Grasp of Multifingered Hand," *Proc. of IEEE Int. Conf. on Robotics and Automation*, pp. 2462-2469, April 1996.

[4] V. Nguyen, "Constructing Force-Closure Grasps in 3-D," *Proc. of IEEE Int. Conf. on Robotics and Automation*, pp. 240-245, March 1987.

[5] K. Yoloi, M. Kaneko, and K. Tanie, "A Compliance Control Method Suggested by Muscle Networks In Human Arms," *Proc. of IEEE/RSJ Int. Conf. on Intelligent Robots and Systems*, pp. 385-390, 1988.

[6] M. R. Cutkosky, and I. Kao, "Computing and controlling the compliance of a robotic hand," *IEEE Trans. on Robotics and Automation*, Vol. 5, No. 2, pp. 151-165, 1989.

[7] Y. T. Lee, H. -R Choi, W. K. Chung, and Y. Youm, "Stiffness Control of a Coupled Tendon-Driven Robot Hand," *IEEE Control Systems Magazine*, Vol. 14, No. 5, pp. 10-19, Oct. 1994.

[8] B. -H. Kim, B. -J. Yi, I. H. Suh, and S. -R. Oh, "A Biomimetic Compliance Control of Robot Hand by Considering Structures of Human Finger," *Proc. of IEEE Int. Conf. on Robotics and Automation*, April 2000.

[9] D. E. Whitney, "Quasi-Static Assembly of Compliantly Supported Rigid Parts," *Jour. of Dynamic systems, Measurement, and control*, Vol. 104, pp. 65-77, March 1982.

[10] H. Asada, Y. Kakumoto, "The Dynamic Analysis and Design of a High-Speed Insertion Hand Using the Generalized Centroid and Virtual Mass," *Jour. of Dynamic systems, Measurement, and control*, Vol. 112, pp. 646-652, 1990.

[11] T. Matsuoka, T. Hasegawa, T. Kiriki, and K, Honda, "Mechanical Assembly based on Motion Primitives of Multi-fingered Hand," *Proc. of Advanced Intelligent Mechatronics*, 1997.

[12] K. B. Shimoga and A. A. Goldenberg, "Grasp Admittance Center: Choosing Admittance Center Parameters," *Proc. of American Control Conference*, pp. 2527-2532, 1991.

[13] B. -J. Yi, I. H. Suh, and S. -R. Oh, "Analysis of a five-bar finger mechanism having redundant actuators with applications to stiffness and frequency modulation," *Proc. of IEEE Int. Conf. on Robotics and Automation*, pp. 759-765, 1997.